

# Effect of Substitutional Impurities on the Electronic States and Conductivity of Crystals with Half-filled Band

E. P. Nakhmedov<sup>1,2</sup>, H. Feldmann<sup>1</sup>, R. Oppermann<sup>1</sup> and M. Kumru<sup>3</sup>

<sup>1</sup>*Institut für Theoretische Physik, Universität Würzburg, 97074 Würzburg, F.R.Germany*

<sup>2</sup>*Azerbaijan Academy of Sciences, Institute of Physics, H. Cavid St. 33, Baku, Azerbaijan*

<sup>3</sup>*Fatih University, Büyükcemece, Istanbul, Turkey*

(October 26, 2018)

Low temperature quantum corrections to the density of states (DOS) and the conductivity are examined for a two-dimensional(2D) square crystal with substitutional impurities. By summing the leading logarithmic corrections to the DOS its energy dependence near half-filling is obtained. It is shown that substitutional impurities do not suppress the van Hove singularity at the middle of the band, however they change its energy dependence strongly.

Weak disorder due to substitutional impurities in the three-dimensional simple cubic lattice results in a shallow dip in the center of the band.

The calculation of quantum corrections to the conductivity of a 2D lattice shows that the well-known logarithmic localization correction exists for all band fillings. Furthermore the magnitude of the correction increases as half-filling is approached. The evaluation of the obtained analytical results shows evidence for delocalized states in the center of the band of a 2D lattice with substitutional impurities.

73.20.Fz; 73.50.-h; 73.20.Dx; 73.50.Bk; 73.20.Jc

## I. INTRODUCTION

The investigation of effects of weak localization in low-dimensional electronic systems still preserves its popularity today, since experimental studies of these systems give occasionally surprising results like metal-insulator phase transitions in the two-dimensional (2D) electron gas at zero magnetic field<sup>1</sup> and unusual behavior of dephasing time in quasi one-dimensional metallic wires<sup>2</sup> at low temperatures. Impurity effects in one-dimensional (1D) disordered systems have been studied accurately due to the existence of methods which give exact results for the cases of both weak and strong disorder.<sup>3,4</sup> Also perturbative approaches give good results for three-dimensional (3D) weakly disordered systems.

Weak localization corrections to the kinetic coefficients of 2D disordered systems are logarithmically divergent corrections and it is hard to sum perturbatively the leading divergent contributions. The dimension two is the marginal dimension for the localization problem and a small external perturbation can change the character of localization in these systems.

According to the scaling theory of Abrahams *et. al.*<sup>4</sup> all states of 1D and 2D electronic gases moving in the field of randomly distributed impurities are completely localized irrespective of the degree of randomness, and in 3D the Anderson metal-insulator phase transition occurs with increasing impurity concentration. Notice that the result of the scaling theory for 1D disordered systems is in agreement with exact results.<sup>5,6</sup> The scaling theory, and also the diagrammatic approach to the problem for 2D weakly disordered systems has revealed logarithmic quantum corrections to the conductivity,<sup>7</sup> which tend towards localization. The logarithmic correction to the conductivity found in [4,7] can be expressed as

$$\sigma - \sigma_0 = -\frac{e^2}{2\pi^2} \ln \frac{\tau^*}{\tau} \quad (1)$$

where  $\sigma_0$  is the Drude conductivity,  $\tau^* = \min\{\tau_\varphi, \frac{L}{v_F}, \frac{1}{\omega}\}$  with  $\tau$  and  $\tau_\varphi$  being the elastic and inelastic scattering times, respectively;  $L$  is the linear size of a 2D system and  $\omega$  is the external frequency.

Notice that weak disorder gives no singular contribution to the density of states (DOS)  $\rho(\epsilon)$  of electron gas models when the condition  $p_F l \gg 1$  or  $\epsilon_F \tau \gg 1$  is satisfied ( $p_F$  and  $\epsilon_F$  are the Fermi momentum and the Fermi energy;  $l$  is the mean free path). According to the Einstein relation  $\sigma = e^2 \rho D$  the quantum correction Eq.(1) to  $\sigma$  is due to changes in the diffusion coefficient<sup>7,8</sup>  $D$ .

Even short-range and weak correlations in weakly disordered metals have been shown<sup>8-11</sup> to result in nontrivial quantum corrections to the DOS of low-dimensional conductors near the Fermi level. Electron-electron interactions in disordered systems also give rise to quantum corrections to the conductivity, which tend to localize the electronic

states. Further, the DOS of strongly doped semiconductors in the presence of long range Coulomb interaction vanishes at the Fermi surface,<sup>12–14</sup> which is commonly referred to as Coulomb gap.

Disordered metals in most of the papers on localization problems are modeled as a free electron gas moving in the random field of impurities. However, doped crystals with low concentrations of impurities usually preserve their periodical structures and the impurity atoms in most cases substitute the host atoms of the lattice. Substitutional impurities appear to have strong influence on the physical properties of low-dimensional lattices near the commensurate values of the electron wave length  $\lambda$  with the lattice constant  $a$  [ 15].

In this paper we shall study the effects of substitutional impurities with small concentration on the density of states and the conductivity of a 2D square lattice. The effects of commensurability on the DOS for the 3D simple cubic lattice will also be considered for the sake of completeness.

Bragg reflections of the electronic wave on the Brillouin zone boundary in the process of impurity scattering become essential as the middle of the band is approached. This process introduces a new relaxation time for umklapp scattering to the problem, which increases for a deviation from half-filling due to the distortion of the commensurability condition for the Bragg reflection.

The lattices under consideration have square structure for 2D and simple cubic structure for 3D crystals. Our calculations show that umklapp scattering strongly changes the energy dependence of the DOS close to half-filling, causing it to decrease. For the 2D square lattice the DOS of the pure system has a logarithmic van Hove singularity at the middle of the band. This peak is shown to be preserved for the lattice with substitutional impurities. However its energy dependence is changed strongly, and the peak becomes narrower.<sup>15</sup> For the 3D lattice, the van Hove singularities lie far from the center of the band and umklapp scattering forms a shallow dip on the Fermi surface, the depth of which increases with the impurity concentration.

Periodicity causes the appearance of a new class of diagrams which give a contribution to the conductivity  $\sigma(\omega)$ . These corrections to the conductivity can be separated into two classes: corrections due to the diffusion coefficient and due to the DOS. Although quantum corrections to the diffusion coefficient slightly increase  $\sigma(\omega)$ , the total corrections sum up to a decrease of  $\sigma(\omega)$  due to DOS corrections in the vicinity of half-filling.

The paper is structured in the following form. In Sec.II the method is described, where new diffusion and cooperon blocks due to umklapp scattering are introduced and calculated. Sec.III is devoted to the calculation of corrections to the DOS near half-filling for 2D and 3D lattices. In Sec.IV, the calculation of the conductivity of the 2D square lattice with substitutional impurities is presented. In Sec.V, a conclusion and a discussion of the results are given.

## II. DESCRIPTION OF THE METHOD

The Hamiltonian of a  $d$ -dimensional simple cubic lattice with substitutional impurities is given by

$$\hat{H} = \hat{H}_0 + V(\mathbf{r}) \quad (2)$$

where  $\hat{H}_0$  is the tight-binding Hamiltonian of noninteracting electrons in a regular lattice with lattice constant  $a$  and nearest-neighbor hopping;  $V(\mathbf{r}) = \sum_i U(\mathbf{r} - \mathbf{R}_i)$  is the impurity potential with  $\mathbf{R}_i$  being the positional vector of an impurity randomly located on the  $i$ -th lattice site.

By introducing the second quantization operators  $c_{\mathbf{p},\sigma}^\dagger$  and  $c_{\mathbf{p},\sigma}$  for an electron with momentum  $\mathbf{p}$  and spin  $\sigma$ , Eq.(2) can be rewritten as

$$\hat{H} = \sum_{\mathbf{p},\sigma} \epsilon(\mathbf{p}) c_{\mathbf{p},\sigma}^\dagger c_{\mathbf{p},\sigma} + \sum_{\mathbf{p},\mathbf{q},\mathbf{G},\sigma} \rho_{\text{imp}}(\mathbf{q}) U(\mathbf{q}) c_{\mathbf{p},\sigma}^\dagger c_{\mathbf{p}+\mathbf{q}+\mathbf{G},\sigma} \quad (3)$$

where  $\rho_{\text{imp}}(\mathbf{q}) = L^{-d} \sum_i \exp(i\mathbf{q}\mathbf{R}_i)$  and  $U(\mathbf{q})$  is the Fourier transform of a single impurity potential. Throughout this paper, we work in units of  $\hbar = 1$ . The momenta  $\mathbf{p}$  and  $\mathbf{q}$  vary in the first Brillouin zone and  $\mathbf{G}$  is a reciprocal lattice vector.  $\epsilon(\mathbf{p})$  in Eq.(3) is the energy spectrum of an electron on a  $d$ -dimensional square lattice,

$$\epsilon(\mathbf{p}) = t[2 - \cos(p_x a) - \cos(p_y a)] \quad \text{for } d = 2 \quad (4)$$

$$\epsilon(\mathbf{p}) = t[3 - \cos(p_x a) - \cos(p_y a) - \cos(p_z a)] \quad \text{for } d = 3 \quad (5)$$

where  $p_{x,y,z} = \frac{2\pi}{aN_{x,y,z}} n_{x,y,z}$  with  $\frac{-N_{x,y,z}}{2} < n_{x,y,z} \leq \frac{N_{x,y,z}}{2}$  and  $t$  is the tunneling integral for nearest-neighbor sites.

The electronic bandwidth is  $W = 4t$  for  $d = 2$  and  $W = 6t$  for 3D systems. As half-filling is approached, which corresponds to  $\epsilon_F = 2t$  for 2D and  $\epsilon_F = 3t$  for 3D system, the Fermi surface becomes nested, i.e. it exhibits surface elements which can be mapped onto each other through one nesting vector. In our case, the nesting condition is satisfied for all parts of the surface, and for 2D square lattices, the Fermi surface at half-filling is flat (see Fig.1).

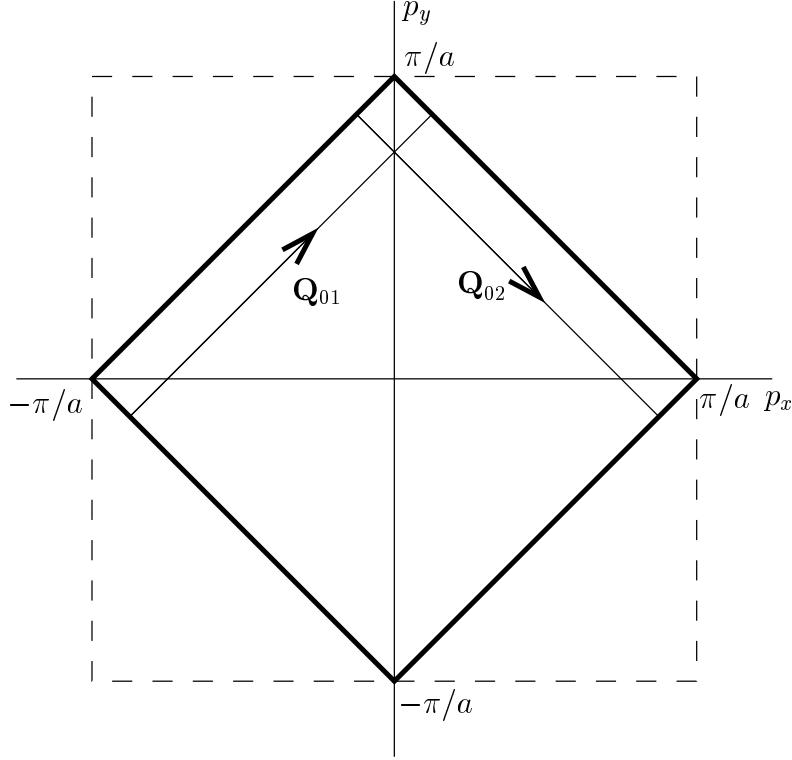


FIG. 1. Fermi surface of a square lattice with nearest-neighbor hopping at half-filling. Complete nesting occurs with the nesting vectors  $\mathbf{Q}_0 = \pm\mathbf{Q}_{01}; \pm\mathbf{Q}_{02}$ , where  $\mathbf{Q}_{01} = \{\frac{\pi}{a}, \frac{\pi}{a}\}$  and  $\mathbf{Q}_{02} = \{-\frac{\pi}{a}, \frac{\pi}{a}\}$  are shown in the figure.

The second part of the Hamiltonian  $\hat{H}$  in Eq.(3), which describes an electron scattering on randomly distributed impurities, contains both normal (for  $\mathbf{G} = 0$ ) and umklapp (for  $\mathbf{G} \neq 0$ ) processes. The impurity concentration is assumed to be small, so that the Born approximation is appropriate<sup>16</sup> to estimate the scattering process on the impurities. The impurity potential in this case is chosen to be a  $\delta$ -correlated Gaussian potential with zero average value.

Conventional diagrammatic techniques<sup>16</sup> are applied to calculate the effects of umklapp scattering on the DOS and the conductivity. The bare Green's functions  $G_{R,A}^0(\epsilon, \mathbf{p})$  at zero temperature are given as

$$G_{R,A}^0(\epsilon, \mathbf{p}) = \frac{1}{\epsilon - (\epsilon(\mathbf{p}) - \epsilon_F) + \frac{i}{2\tau} \text{sign}\epsilon} \quad (6)$$

where  $\epsilon > 0$  and  $\epsilon < 0$  correspond to retarded  $G_R^0$  and advanced  $G_A^0$  Green's functions, respectively. The energy spectrum  $\epsilon(\mathbf{p})$  in Eq.(6) is expressed by Eqs.(4) and (5) for 2D and 3D cases, respectively. For momenta lying close to the Fermi surface (in the first Brillouin zone) the energy spectrum can be linearized around the Fermi surface and  $\epsilon(\mathbf{p}) - \epsilon_F \approx \mathbf{v}_F(\mathbf{p} - \mathbf{p}_F) = v_F(|\mathbf{p}| - p_F) \cos \alpha$ , where  $\mathbf{v}(\mathbf{p}) = \frac{\partial \epsilon}{\partial \mathbf{p}} = at\{\sin p_x a, \sin p_y a\}$  is the group velocity of the electron wave packet. In contrast to the electron gas model the linearized energy spectrum contains the additional parameter  $\cos \alpha$  due to non-collinearity of the momentum and velocity vectors. For small band filling, the Fermi surface is very similar to a sphere, so this factor can be set equal to unity. Approaching half-filling, this parameter becomes weakly varied, e.g.  $\frac{1}{\sqrt{2}} \leq \cos \alpha \leq 1$  for a 2D system at half-filling, where the range of variation of  $\cos \alpha$  is maximal. As an approximation, we can always set  $\cos \alpha = 1$ . In the vicinity of commensurate points, especially at half-filling, electron scattering on impurities with large momentum transfer involves umklapp processes. The procedure of expansion of the energy spectrum around the Fermi surface can in this case be performed after the separation of the large momentum transfer  $\mathbf{Q}_0$ .

In weak localization theory the maximally crossed diagrams are responsible for the low temperature quantum corrections to the kinetic properties of low-dimensional disordered systems, modeled as an electron gas moving in the field of randomly distributed impurities<sup>7</sup>. These diagrams can be redrawn as ladder diagrams in a particle-particle channel (Fig.2a). The cooperon block has a pole for small total momentum of particles,  $|\mathbf{q}|l \ll 1$ , and for small energy difference  $|\omega|\tau \ll 1$ . The cooperon block turns out to have a diffusion pole also for large momentum transfer when the total momenta of the particles are  $(\mathbf{Q}_0 + \mathbf{q})$  with  $|\mathbf{q}|l \ll 1$  and when the total energy is small. In this case each

act of scattering on an impurities involves a large momentum transfer close to  $\mathbf{Q}_0$ . This process of course takes place mainly around half-filling when  $\mathbf{Q}_0 = 2\mathbf{p}_F$ , and it consists of simultaneous Bragg reflection of the electron in the process of scattering on the impurity, with relaxation time  $\tau_\pi$ . This scattering process will be further referred to as  $\pi$ -scattering.

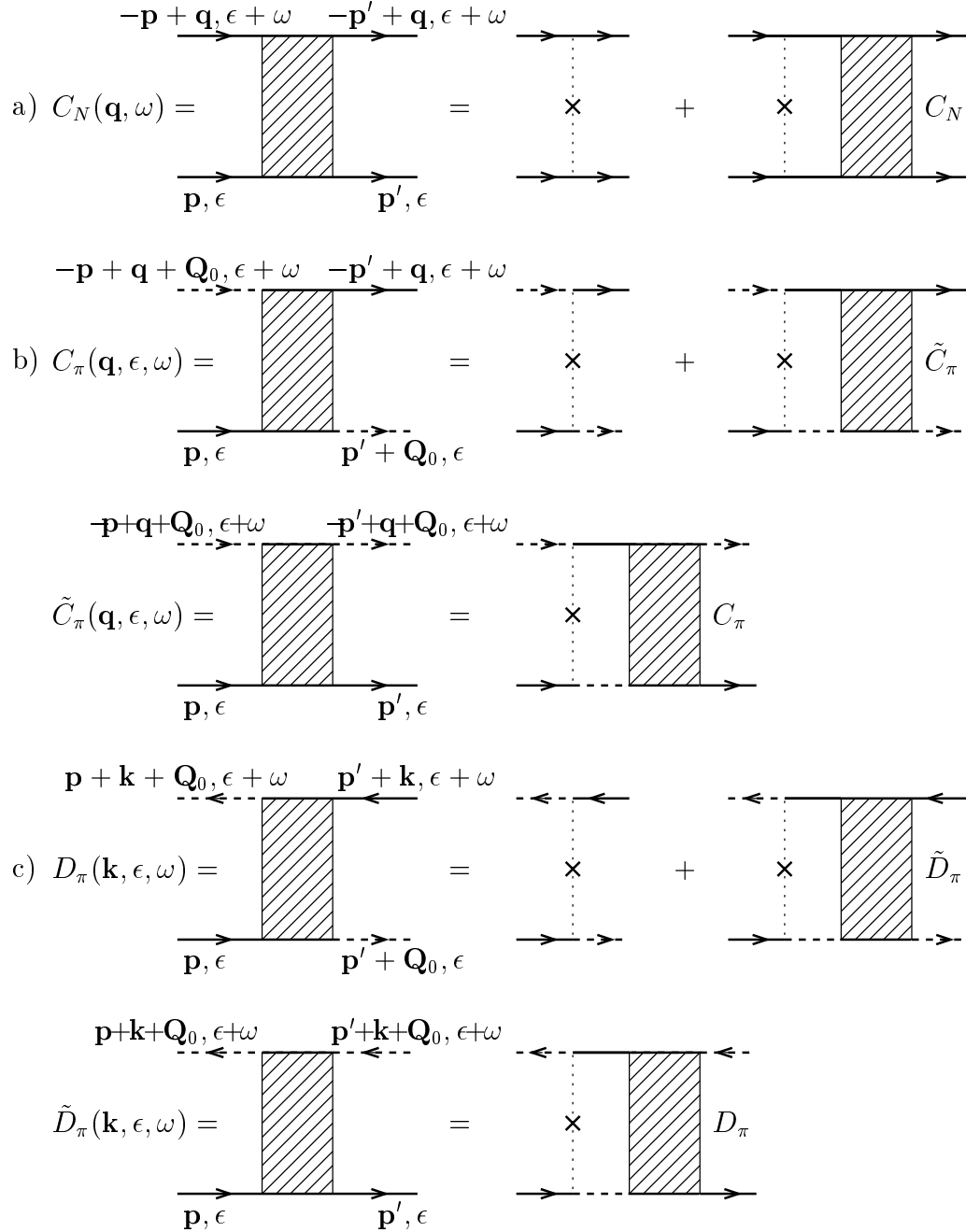


FIG. 2. The ladder series for a) the normal cooperon  $C_N$ , b) the  $\pi$ -cooperon  $C_\pi$  and c) the  $\pi$ -diffuson  $D_\pi$ . In b) and c),  $\tilde{C}_\pi$  and  $\tilde{D}_\pi$  are expressed by  $\tilde{C}_\pi = J_\pi C_\pi$  and  $\tilde{D}_\pi = J_\pi D_\pi$ , where  $J_\pi$  is given in Eq.(11).

Two different scattering processes and corresponding relaxation times can be separated: Normal scattering with  $\tau_N$  (see Fig.3a), when the scattering on an impurity maintains the electron's momentum inside the first Brillouin zone after scattering and  $\pi$ -scattering, with a relaxation time  $\tau_\pi$  (Fig.3b). Here, momentum conservation is violated and this scattering process corresponds to an umklapp process. The total relaxation time  $\tau$  can then be expressed as  $\frac{1}{\tau} = \frac{1}{\tau_N} + \frac{1}{\tau_\pi}$ . Notice here that the expression for the normal relaxation time  $\tau_N$  according to Fig.3a for the 2D case

can be given as

$$\frac{1}{\tau_N} = \frac{C_{\text{imp}}}{(2\pi)^2} \int_S \frac{d\mathbf{S}}{|\mathbf{v}_\mathbf{k}|} |U(\mathbf{p}_F, \mathbf{S})|^2 \quad (7)$$

We assume  $\tau_N$  to be constant and independent of the band filling. This means that the singularities of the integrand due to vanishing velocity at the saddle points are compensated by appropriate zeros of the impurity potential.

To illustrate diagrammatically the impurity scattering including umklapp processes we represent the Green's function of an electron with large momentum by a dashed line. The ladder series for the cooperon block with large momentum transfer,  $C_\pi(\mathbf{q}, \epsilon)$ , is diagrammatically shown in Fig.2b. Notice here that the vertices c) and d) in Fig.3 are irrelevant for the cooperon blocks  $C_\pi(\mathbf{q}, \epsilon)$  and  $C_N(\mathbf{q}, \epsilon)$  (Fig. 2a,b). Indeed, the dashed line alone has no physical meaning, it has only meaning for an electron scattering with large momentum transfer. In ladders, the vertices c) and d) of Fig.3 can always be transformed into normal vertices or those of Fig.3b by proper redefinition of the internal momenta.

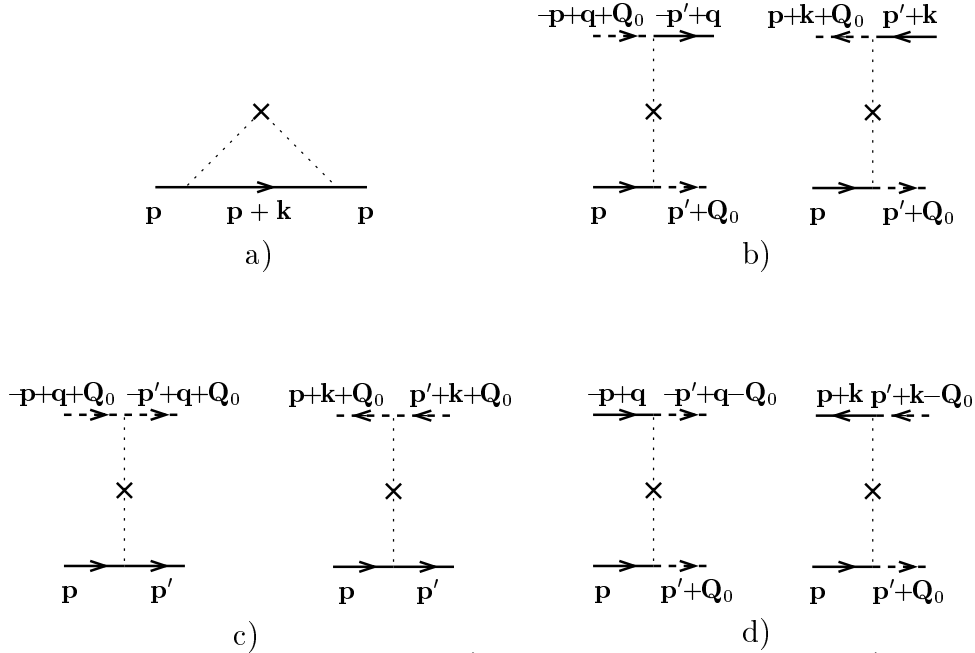


FIG. 3. Impurity vertices which give a contribution to a) the normal relaxation time  $\tau_N$ , b) the relaxation time for  $\pi$ -scattering  $\tau_\pi$ . The vertices c) and d) do not give a contribution to  $\pi$ -scattering.

In the process of propagation in the particle-particle channel the momenta of the particles for the normal cooperon block  $C_N(\mathbf{q}, \omega)$  lie on opposite sites of the Fermi surface during the diffusion process. In contrast to this, the momenta for the two particle propagator  $C_\pi(\mathbf{q}, \epsilon)$  with umklapp process lie on the same section of the Fermi surface and each act of impurity scattering coherently relocates the particles to the opposite section of the Fermi surface due to Bragg reflection. We will refer to this two-particle propagator  $C_\pi(\mathbf{q}, \epsilon)$  as  $\pi$ -cooperon.

The same situation occurs for the  $\pi$ -diffusion block  $D_\pi(\mathbf{k}, \epsilon, \omega)$  (Fig.2) with a large difference  $(\mathbf{Q}_0 + \mathbf{k})$  of electron and hole momenta, with  $|\mathbf{k}|l \ll 1$ . The comparison of the normal diffuson block  $D_N(\mathbf{k}, \epsilon, \omega)$  with the  $\pi$ -diffuson  $D_\pi(\mathbf{k}, \epsilon, \omega)$  reveals again strong differences between these two processes. In the process of propagation in the  $N$ -diffusion channel, electron and hole lie close to each other on the Fermi surface, with momenta  $\mathbf{p}$  and  $\mathbf{p} + \mathbf{k}$ , and  $|\mathbf{k}|l \ll 1$ . They diffuse on the Fermi surface and keep the proximity of the momenta after each act of scattering. In contrast to this, the momenta of electron and hole for the  $\pi$ -diffuson block  $D_\pi$  are located on opposite sides of the Fermi surface. Each scattering on the impurities interchanges the positions of electron and hole on the Fermi surface. Now let us sum the series shown in Fig.2 for  $C_N$ ,  $C_\pi$ , and  $D_\pi$ .

Summing up the ladder series in Fig.2a, the following expression for  $C_N(\mathbf{q}, \omega)$  is obtained:

$$C_N(\mathbf{q}, \omega) = C_{\text{imp}} |U(0)|^2 \left\{ \frac{\sqrt{(1 - i\tau|\omega|)^2 + (ql)^2}}{\sqrt{(1 - i\tau|\omega|)^2 + (ql)^2} - \frac{\tau}{\tau_N}} \Theta(-\epsilon(\epsilon + \omega)) + \Theta(\epsilon(\epsilon + \omega)) \right\} \quad (8)$$

Far from half-filled electronic band,  $\tau_\pi \gg \tau_N$  and  $\tau \approx \tau_N$ . Therefore,  $C_N(\mathbf{q}, \omega)$  has a diffusion pole for  $|\omega|\tau \ll 1$  and  $|\mathbf{q}|l \ll 1$ . As half-filling is approached, umklapp scattering is intensified and  $\tau_\pi \ll \tau_N$  and  $\tau \approx \tau_\pi$ . As a result,

the diffusion pole of  $C_N(\mathbf{q}, \epsilon)$  disappears at half-filling. In this regime, the Fermi surface of the square or simple cubic crystal becomes nested (see Fig.1 for the 2D case) with a nesting vector  $\mathbf{Q}_0 = \{\pm \frac{\pi}{a}, \pm \frac{\pi}{a}\}$  for the 2D lattice and  $\mathbf{Q}_0 = \{\pm \frac{\pi}{a}, \pm \frac{\pi}{a}, \pm \frac{\pi}{a}\}$  for the 3D lattice. In this case, the following particle-hole symmetry of the electron dispersion with respect to the vector  $\mathbf{Q}_0$  holds for the half-filled band:

$$\epsilon(\mathbf{p} + \mathbf{Q}_0) - \epsilon_F = -[\epsilon(\mathbf{p}) - \epsilon_F] \quad (9)$$

The main contribution to the low temperature properties now gives the  $\pi$ -cooperon  $C_\pi(\mathbf{q}, \epsilon, \omega)$  in Fig.2b. One gets the following expression for  $C_\pi(\mathbf{q}, \epsilon, \omega)$  by summing the ladder series in Fig.2:

$$C_\pi(\mathbf{q}, \epsilon, \omega) = C_{\text{imp}} |U|^2 \frac{J_\pi^2}{1 - J_\pi^2} \quad (10)$$

where  $J_\pi$  is the expression for an elementary “bubble” in the ladder series and

$$J_\pi = C_{\text{imp}} \int \frac{d^d p}{(2\pi)^d} |U|^2 G(\mathbf{p}, \epsilon), G(-\mathbf{p} + \mathbf{q} + \mathbf{Q}_0, \epsilon + \omega) \quad (11)$$

To calculate  $J_\pi$ , the large momentum  $\mathbf{Q}_0$  is removed using the electron-hole symmetry relation Eq.(9), and after this the energy spectrum is linearized around the Fermi surface. As a result we get the following expression for  $C_\pi(\mathbf{q}, \epsilon, \omega)$ :

$$C_\pi(\mathbf{q}, \epsilon, \omega) = C_{\text{imp}} |U(2p_F)|^2 \left\{ \frac{(\tau/\tau_\pi)^2}{(1 - i\tau|2\epsilon + \omega|)^2 + (ql)^2 - (\tau/\tau_\pi)^2} \Theta(\epsilon(\epsilon + \omega)) + \Theta(-\epsilon(\epsilon + \omega)) \right\} \quad (12)$$

So the  $\pi$ -cooperon has a diffusion pole for total momenta close to  $\mathbf{Q}_0$  ( $|\mathbf{k}| \ll 1$ ) and small total energy  $|2\epsilon + \omega|\tau \ll 1$  of the particles. The diffusion block  $D_\pi(\mathbf{k}, \epsilon, \omega)$ , which differs from  $C_\pi(\mathbf{q}, \epsilon, \omega)$  through time reversal of one electron line, has a pole for large  $(\mathbf{Q}_0 + \mathbf{k})$  momenta difference with  $|\mathbf{k}| \ll 1$  and small total energy of electron and hole (see Fig.2c). The calculation of  $D_\pi(\mathbf{k}, \epsilon, \omega)$  is similar to that for  $C_\pi(\mathbf{q}, \epsilon, \omega)$  and we obtain

$$D_\pi(\mathbf{k}, \epsilon, \omega) = C_{\text{imp}} |U(2p_F)|^2 \left\{ \frac{(\tau/\tau_\pi)^2}{(1 - i\tau|2\epsilon + \omega|)^2 + (kl)^2 - (\tau/\tau_\pi)^2} \Theta(\epsilon(\epsilon + \omega)) + \Theta(-\epsilon(\epsilon + \omega)) \right\} \quad (13)$$

After this, we can calculate the corrections to the DOS and the conductivity due to umklapp processes.

### III. DENSITY OF STATES AT HALF-FILLING

The one-particle DOS of the regular  $d$ -dimensional lattice is expressed as

$$\rho_0^{(d)} = \frac{2}{(2\pi)^d} \int_S \frac{d\mathbf{S}}{|\nabla \epsilon(\mathbf{k})|} \quad (14)$$

where  $d\mathbf{S}$  is an element of an isoenergetic surface in  $d$ -dimensional space.  $\rho_0^{(d)}$  has a van Hove singularity at the points where the group velocity of the electron wave packet  $\mathbf{v}_k = \nabla \epsilon(\mathbf{k})$  vanishes.<sup>17</sup>

The DOS of a clean 1D lattice with constant spacing  $a$  is easily calculated to be  $\rho_0^{(1)} = \frac{1}{\pi a \sqrt{\epsilon(2t - \epsilon)}}$ . This expression shows that  $\rho_0^{(1)}$  is a regular function of the energy near half-filling when  $\epsilon \rightarrow \epsilon_F = t$  and it has a power-like singularity when  $\epsilon$  approaches the band edges  $\epsilon \rightarrow 0, 2t$ . The bare DOS of a 2D crystal with an energy spectrum given by Eq.(4) has a logarithmic van Hove singularity in the middle of the band:

$$\rho_0^{(2)} = \frac{1}{\pi^2 a^2 t} K\left(\sqrt{1 - \left(\frac{\epsilon}{2t}\right)^2}\right) = \begin{cases} \frac{2}{\pi a^2 \sqrt{4t^2 - \epsilon^2}} \ln \frac{4t^2 - \epsilon^2}{\epsilon^2} & \text{for } |\epsilon| \ll 2t \\ \frac{1}{\pi a^2 |\epsilon|} & \text{for } |\epsilon| \approx 2t \end{cases} \quad (15)$$

Here and below, the electron energy  $\epsilon$  is measured from the middle of the band, i.e.  $\epsilon = 0$  corresponds to half-filling. The van Hove singularity of simple 3D crystals with nearest-neighbor hopping exhibits cusps near  $|\epsilon| = t$ :

$$\rho_0^{(3)} = \text{const} - \frac{2}{\pi^2 t^{3/2} a^3} \sqrt{\epsilon - t} \quad (16)$$

In this section we will study effects of substitutional impurities on the DOS of 2D and 3D crystals. Randomly distributed impurities in  $d$ -dimensional electron gases have no effect on the DOS.

The DOS of 2D and 3D simple (cubic) crystals with substitutional impurities turns out to have a quantum correction near the middle of the band even for noninteracting electrons. Effects of commensurability on the DOS and on the kinetics of 1D disordered crystals near the middle of the band have been calculated by many authors.<sup>18–26</sup> Dyson first pointed out<sup>18</sup> that the DOS of phonons of a 1D disordered chain has a singularity as  $\rho^{(1)} \propto -|\epsilon|^{-1} \ln^{-3} |\epsilon|$  near the middle of the band. Notice that the singular increasing of the DOS in a 1D system at half-filling is not connected with the van Hove singularity, since the latter is located at the band edge for the 1D system. Instead it is mediated by the interference of impurity scattering and Bragg reflections at half-filling. Later an analogous singularity has been found in the electronic DOS of many 1D models.<sup>19–26</sup> Since the 1D scattering problem is characterized by forward and backward scattering processes, 1D models with off-diagonal disorder display a singularity at the center of the band only if the forward scattering amplitude turns to zero. Small forward scattering with Bragg reflection seems to enhance localization and as a result the DOS divergence in the band center is blurred.

Effects of substitutional impurities on the DOS of 2D (square, honeycomb and triangular) and 3D (simple cubic) lattices have been studied computationally<sup>27–29</sup> for cases with diagonal and off-diagonal disorder. The existence of a van Hove singularity in the DOS of a two sublattice model for  $d \geq 2$  has been shown in [30] on the basis of an  $\frac{1}{n}$  expansion in disordered systems with  $n$  orbitals per site for energies approaching the band center. In all cases diagonal disorder has been shown to suppress the van Hove singularity, whereas it is preserved for the 2D simple square lattice with off-diagonal disorder.

We start from the following expression for the DOS

$$\rho^{(d)}(\epsilon) = -\frac{2}{\pi} \text{Im} \int \frac{d^d p}{(2\pi)^d} G_R(\mathbf{p}, \epsilon) \quad (17)$$

which expresses  $\rho(\epsilon)$  by means of the retarded Green's function  $G_R(\mathbf{p}, \epsilon)$ . The new class of diagrams which give the dominating contribution to the self-energy of  $G_R(\mathbf{p}, \epsilon)$  is drawn in Fig.4.

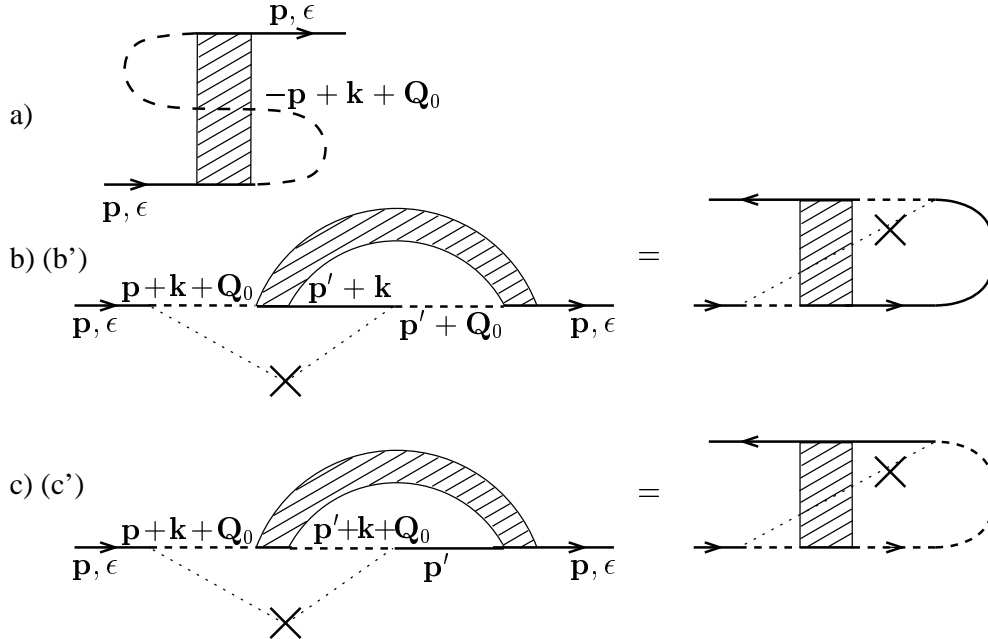


FIG. 4. Self energy parts which give the leading contributions to the Green's function due to umklapp scattering in a) cooperon and b,c) diffuson channels. Diagrams symmetrically conjugate to b) and c) with respect to the impurity line, also give a contribution to the self-energy.

These diagrams represent the contributions to the self-energy in first order in cooperon and diffuson blocks ( $C_\pi(\mathbf{q}, \epsilon)$  and  $D_\pi(\mathbf{k}, \epsilon)$ ). Since  $C_\pi(\mathbf{q}, \epsilon)$  and  $D_\pi(\mathbf{k}, \epsilon)$  do not carry an external frequency ( $\omega = 0$ ), their expressions are obtained from Eqs.(12) and (13) with  $\omega = 0$ :

$$C_\pi(\mathbf{q}, \epsilon) = C_{\text{imp}} |U(2p_F)|^2 \left(\frac{\tau}{\tau_\pi}\right)^2 \frac{1}{(1 - 2i\tau|\epsilon|)^2 + (ql)^2 - (\tau/\tau_\pi)^2} \quad (18)$$

$$D_\pi(\mathbf{k}, \epsilon) = C_{\text{imp}} |U(2p_F)|^2 \left(\frac{\tau}{\tau_\pi}\right)^2 \frac{1}{(1 - 2i\tau|\epsilon|)^2 + (kl)^2 - (\tau/\tau_\pi)^2} \quad (19)$$

As  $\tau_\pi \rightarrow \tau$ , both blocks have a diffusion pole for  $|\epsilon|\tau \ll 1$  and  $ql, kl \ll 1$ . The cooperon and the diffuson blocks give rise to logarithmic corrections to the physical parameters for  $d = 2$  and  $\sqrt{|\epsilon|\tau}$  corrections for  $d = 3$ . Therefore, diagrams of higher order in the cooperon and diffuson blocks for the self-energy parts are not necessary for 3D systems for  $|\epsilon|\tau \ll 1$ . Nevertheless the logarithmic divergency existing in the first order contribution to the self-energy for 2D systems requires to examine higher order logarithmic corrections. The structure of the diagrams which contain all possible combinations of diffuson and cooperon blocks becomes complicated with increasing number of inserted blocks.

However, as it has been shown by various theoretical methods, higher logarithmic corrections to the conductance cancel each other<sup>7,31,30</sup> and the leading correction to the conductance is only the first order logarithmic term.

High order corrections to the self-energy seem to cancel each other also in our case. The second order diagrams which give logarithm-squared contributions to the self-energy are drawn in Fig.5. Straightforward calculations show that the sum of these diagrams gives zero.

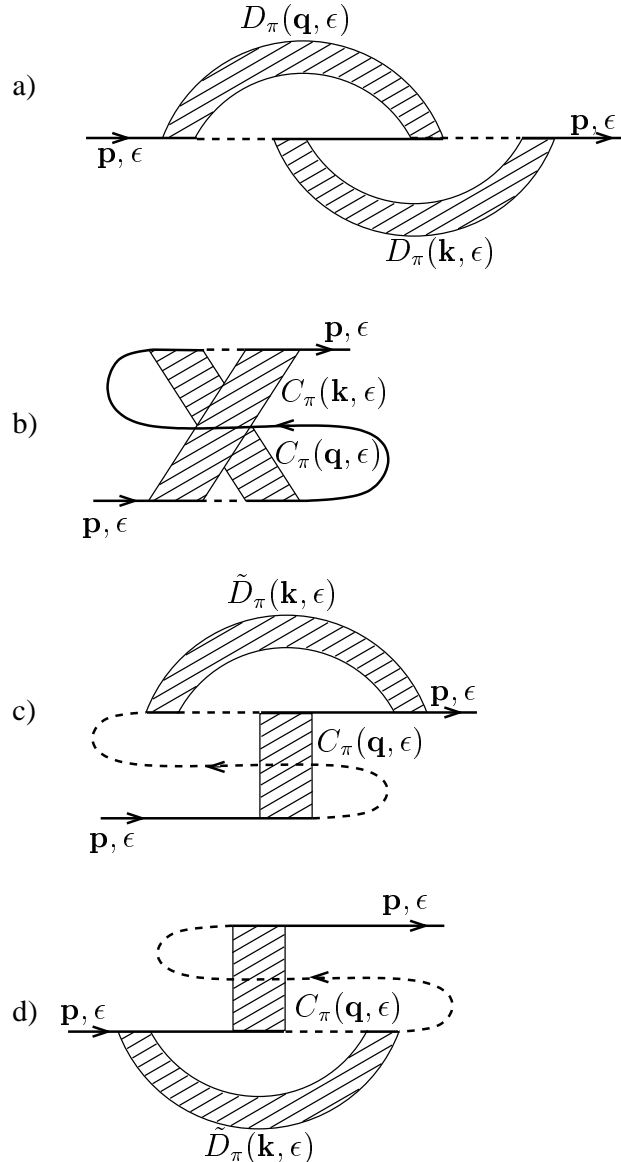




FIG. 5. Contributions of second order in cooperon and diffuson blocks to the self-energy. The calculations shows a complete cancellation between these diagrams. The second-order self-energy diagrams obtained by mutual insertion of the diagrams of Fig.4, with a total number of 40, also completely cancel each other at half-filling.

The retarded Green's function  $G_R(\epsilon, \mathbf{p})$  is expressed by the sum of the first-order self-energy parts  $\Sigma(\epsilon, \mathbf{p})$  in Fig.4 according to the Dyson equation as

$$G_K(\epsilon, \mathbf{p}) = \frac{1}{(G_R^0(\epsilon, \mathbf{p}))^{-1} - \Sigma(\epsilon, \mathbf{p})} = \sum_{n=0}^{\infty} (G_R^0(\epsilon, \mathbf{p}))^{n+1} (\Sigma(\epsilon, \mathbf{p}))^n \quad (20)$$

By summing the diagrams in Fig.4 one gets the expression for  $\Sigma(\epsilon, \mathbf{p})$ :

$$\Sigma(\epsilon, \mathbf{p}) = \int \frac{d^d k}{(2\pi)^d} \left\{ C_\pi(\epsilon, \mathbf{k}) - \frac{2\tau}{\tau_\pi} \left(1 - \frac{\tau}{\tau_\pi}\right) D_\pi(\epsilon, \mathbf{k}) \right\} G_R^0(-\mathbf{p} + \mathbf{k} + \mathbf{Q}_0, \epsilon) \quad (21)$$

By substituting Eqs.(20) and (21) into Eq.(17) one obtains the following expression for  $\rho(\epsilon)$ :

$$\rho(\epsilon) = \rho_0^{(d)} - \frac{2}{\pi} \text{Im} \sum_{n=1}^{\infty} A_n \alpha_d^n(\epsilon) \quad (22)$$

with

$$\alpha_d(\epsilon) = 4\tau^2 \int \frac{d^d k}{(2\pi)^d} \left\{ C_\pi(\epsilon, \mathbf{k}) - \frac{2\tau}{\tau_\pi} \left(1 - \frac{\tau}{\tau_\pi}\right) D_\pi(\epsilon, \mathbf{k}) \right\} \quad (23)$$

and

$$A_n = \frac{1}{(2\tau)^{2n}} \int \frac{d^d k}{(2\pi)^d} G_0^{n+1}(\epsilon, \mathbf{p}) G_0^n(-\mathbf{p} + \mathbf{p}_0, \epsilon) = (-1)^{n+1} 2\pi i \rho_0^{(d)} \frac{n(2n-1)!}{2^{2n}(n!)^2} \quad (24)$$

Here,  $\rho_0^{(d)}$  is the DOS for a  $d$ -dimensional clean crystal and is given by Eqs.(15) and (16) for  $d = 2$  and  $d = 3$ , respectively. The sum over  $n$  in Eq.(22) is performed easily using Eq.(24):

$$\rho(\epsilon) = \rho_0^{(d)} \left\{ 1 - \text{Re} \frac{\alpha_d(\epsilon)}{\sqrt{1 + \alpha_d(\epsilon)}(1 + \sqrt{1 + \alpha_d(\epsilon)})} \right\} = \rho_0^{(d)} \text{Re} \frac{1}{\sqrt{1 + \alpha_d(\epsilon)}} \quad (25)$$

where the energy dependence of  $\alpha_d(\epsilon)$  is obtained from Eqs.(23), (18) and (19):

$$\alpha_d(\epsilon) = \begin{cases} \frac{1}{2\pi\epsilon_F\tau_\pi} \left(1 - \frac{2\tau}{\tau_\pi} + \frac{2\tau^2}{\tau_\pi^2}\right) \ln \frac{2 - \frac{\tau^2}{\tau_\pi^2}}{1 - \frac{\tau^2}{\tau_\pi^2} - 4i|\epsilon|\tau} & \text{for } d = 2 \\ \frac{3\left(1 - \frac{2\tau}{\tau_\pi} + \frac{2\tau^2}{\tau_\pi^2}\right)}{4\pi\tau\tau_\pi\epsilon_F^2} \left\{ 1 - \frac{\pi\sqrt{3}}{4} \left[ \sqrt{\left(1 - \frac{\tau^2}{\tau_\pi^2}\right)^2 + (4\tau|\epsilon|)^2 - 1 + \frac{\tau^2}{\tau_\pi^2}} \right. \right. \\ \left. \left. - i \sqrt{\left(1 - \frac{\tau^2}{\tau_\pi^2}\right)^2 + (4\tau|\epsilon|)^2 + 1 - \frac{\tau^2}{\tau_\pi^2}} \right] \right\} & \text{for } d = 3 \end{cases} \quad (26)$$

It can be seen from Eqs.(25) and (26) that away from half-filling, the effects of Umklapp scattering are weakened and  $\tau_\pi \gg \tau_N \approx \tau$ , as a result of which the quantum corrections to the DOS disappear. In the vicinity of half-filling,  $\tau \approx \tau_\pi < \tau_N$  and impurity effects become essential.

The DOS for a 2D system with half-filled energy band can be expressed as

$$\rho^{(2)}(\epsilon) = \rho_0^{(2)}(\epsilon) \frac{1}{\sqrt{1 + \frac{1}{2\pi\epsilon_F\tau_\pi} \ln \frac{1}{4|\epsilon|\tau_\pi}}} \quad (27)$$

where  $\rho_0^{(2)}(\epsilon)$ , given by Eq.(15), contains a logarithmic singularity in the middle of the band. Eq.(27) shows that the van Hove singularity in the DOS of a pure 2D square crystal is preserved in the presence of substitutional impurities.

However, the central peak becomes narrower due to impurity scattering than that of the van Hove peak in clean systems. In the vicinity of the band center the energy dependence of  $\rho^{(2)}(\epsilon)$  is changed from logarithmic dependence to the square root of the logarithm,<sup>15</sup>

$$\rho^{(2)}(\epsilon) = \frac{2}{(\pi a)^2 \epsilon_F} (2\pi \epsilon_F \tau_\pi)^{1/2} \ln^{1/2} \left( \frac{1}{4\tau_\pi |\epsilon|} \right) \quad \text{as } |\epsilon| \rightarrow 0 \quad (28)$$

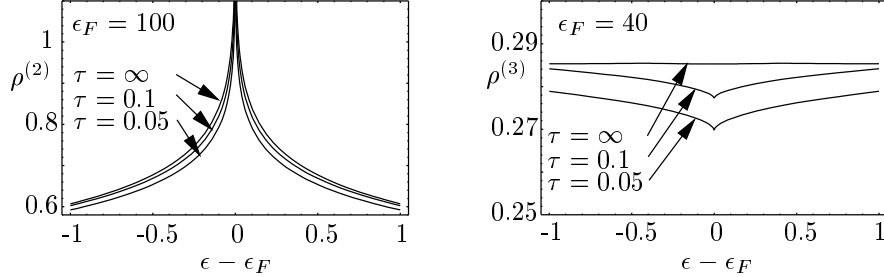


FIG. 6. Impurity effect on  $\rho^{(2)}$  and  $\rho^{(3)}$  for selected values of the impurity potential. The pure DOS  $\rho_0^{(2)}$  and  $\rho_0^{(3)}$ , corresponding to  $\tau = \infty$ , are also given for comparison.

In Fig.6a the dependence of  $\rho^{(2)}(\epsilon)$  on the impurity potential strength is drawn, which displays a narrowing of the central peak with increasing disorder strength or decreasing  $\tau_\pi$ . The DOS of a square lattice with off-diagonal disorder computed in [27,28] shows the same effect. Notice that the impurity potential studied in our problem corresponds to off-diagonal disorder, since the part of the Hamiltonian Eq.(3) corresponding to the impurity potential can be decoupled into diagonal ( $U(\mathbf{0})$ ) and off-diagonal ( $U(\mathbf{q})$  with  $\mathbf{q} \neq 0$ ) parts. The diagonal part is chosen to be equal to zero for the white-noise potential<sup>16</sup> in the averaging process.

Unlike 2D systems, substitutional impurities have small effect on the DOS of 3D simple cubic crystals. In the close vicinity of half-filling, Eq.(23) for  $\alpha_3(\epsilon)$  is simplified:

$$\alpha_3(\epsilon) = \frac{3}{4\pi\tau_\pi^2\epsilon_F^2} \left\{ 1 - \frac{\pi\sqrt{3}}{2} \sqrt{|\epsilon|\tau} (1-i) \right\} \equiv \alpha_R + i\alpha_I \quad (29)$$

By using Eq.(29), one expresses  $\rho^{(3)}(\epsilon)$  as

$$\rho^{(3)}(\epsilon) = \frac{\rho_0^{(3)}}{\sqrt{2}} \frac{\sqrt{1 + \alpha_R + \sqrt{(1 + \alpha_R)^2 + \alpha_I^2}}}{\sqrt{(1 + \alpha_R)^2 + \alpha_I^2}} \approx \frac{\rho_0^{(3)}}{\sqrt{1 + \frac{3}{4\pi\epsilon_F^2\tau_\pi^2} \left( 1 - \frac{\pi\sqrt{3}|\epsilon|\tau}{2} \right)}} \quad (30)$$

where  $\alpha_R(\epsilon)$  and  $\alpha_I(\epsilon)$  are real and imaginary parts of  $\alpha_3(\epsilon)$ , respectively.

Eq.(30) shows that a small dip of the DOS is formed at the middle of a half-filled band of a 3D simple cubic lattice due to substitutional impurities (see Fig.6b). The depth of this dip increases with disorder strength as

$$\rho_0^{(3)}(0) = \frac{\rho_0^{(3)}}{\sqrt{1 + \frac{3}{4\pi\epsilon_F^2\tau_\pi^2}}} \quad (31)$$

The results obtained for the DOS of 2D systems, Eqs.(25)-(28), and 3D systems, Eqs.(29)-(31), show that in contrast to 1D systems substitutional impurities tend to reduce the DOS on the Fermi surface of 2D and 3D crystals at half filling. Indeed, the Dyson singularity, expressing the enhancement of the states density in the 1D lattice with off-diagonal disorder, is mediated by impurities,<sup>18-26</sup> since the DOS of a regular 1D lattice is a smooth function of the energy of a half-filled band.

The mechanism of the relative reduction of the DOS in 2D [Eq.(27)] and 3D [Eq.(30)] systems is Umklapp scattering, the same that increases the 1D DOS. However, the nested Fermi surface of a 2D square crystal with nearest-neighbor hopping contains also saddle points at  $\{\pm\frac{\pi}{a}, 0\}$  and  $\{0, \pm\frac{\pi}{a}\}$  which cause the van Hove singularity in the DOS. Umklapp scattering in this case weakens the central van Hove peak in the DOS, nevertheless it could not damp the peak or reverse its sign. We understand the different effects of substitutional impurities on the DOS of 1D and higher dimensional systems in the following way: The main mechanism of localization in a 1D disordered system is backward

scattering on impurities.<sup>3,5,6</sup> In the process of scattering on an impurity, simultaneous Bragg reflection at half-filling reverses backward scattering to forward scattering and vice versa. Therefore for vanishingly small forward scattering amplitude<sup>20,22</sup> Bragg reflection prevents localization due to impurity scattering. However, the situation is different for 2D and 3D systems. According to the intuitive discussion given by Bergmann,<sup>32</sup> localization in 2D systems is due to interference of the electronic wave, returning to the starting point after multiple scattering on impurities with only a small change of the momentum at each act of scattering, with the wave on the time-reversed path (see also [8]). In this case, the Bragg reflection accompanying the impurity scattering can not destroy the picture of interference and as a result can not completely delocalize all states.

The addition of next-nearest-neighbor hopping terms into the model with strength  $t'$  splits saddle points from the nested Fermi surface. For the energy spectrum  $\epsilon(\mathbf{k}) = -t[\cos p_x a + \cos p_y a - \frac{t'}{t} \cos p_x a \cos p_y a + \frac{\mu}{2}]$  the saddle points again lie at  $\{\pm \frac{\pi}{a}, 0\}$  and  $\{0, \pm \frac{\pi}{a}\}$ . However, the optimal nested Fermi surface is realized at  $t'/t = 0.165$  and  $\mu = -0.56$ , with the new nesting vector  $\mathbf{Q}_0^* = 0.91\mathbf{Q}_0$ .<sup>33</sup> Our method can be applied also for this dispersion band. The singular blocks are again calculated after separating the large momentum transfer  $\mathbf{Q}_0^*$  and linearizing the energy spectrum around the Fermi surface. As a result the same expression (28)) for the 2D DOS is obtained. However,  $\rho_0^{(2)}$  in this case has no singularity on the Fermi surface at half-filling. Therefore  $\rho^{(2)}(\epsilon)$  decreases with the energy around the Fermi surface for half filling and vanishes on it.

#### IV. CONDUCTIVITY

The DC-conductivity for the 2D Anderson model at zero temperature has been computed in [34] and the behavior of  $\sigma$  as a function of the Fermi energy and the disorder has been studied. However, these numerical results provide limited insight into the physical origin of the processes giving contributions to the conductivity. In this section, we study low temperature quantum contributions to the conductivity for the model under consideration. Maximally crossed or “fan” diagrams are responsible for the quantum interference corrections to the conductivity in the weak localization theory.<sup>7</sup> Interference between electronic wave functions in the process of multiple scattering on randomly distributed impurities changes the mobility of an electronic system and “fan” diagrams give a contribution to the diffusion coefficient. The conductivity of simple crystalline systems with substitutional impurities can also be affected through changes in the DOS due to Bragg reflection in the scattering processes on the impurities which becomes essential for an electronic band close to half-filling. The diagrams which describe first order weak localization corrections to the conductivity and represent both the diffusion coefficient and the DOS contributions, are drawn in Fig.7.

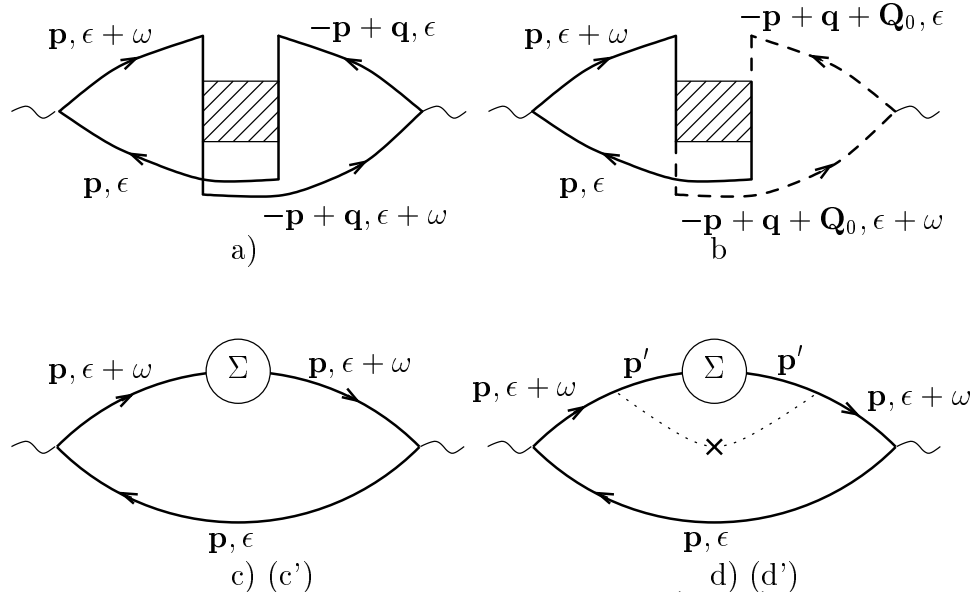


FIG. 7. Diagrams giving the first quantum correction to the conductivity. a) and b) characterize the diffusion coefficient contributions to  $\sigma(\omega)$  from normal and umklapp scattering channels, respectively.  $\Sigma$  in diagrams c)-d), for the contributions from the DOS to  $\sigma(\omega)$ , is the sum of all self-energy contributions shown in Fig.4. Two other diagrams c') and d') differ from c) and d) through the direction of the electron lines.

Since interference effects are essential for low-dimensional systems, we here will calculate the quantum corrections

to the conductivity only for a 2D square lattice with substitutional impurities. The localization problem for a 1D lattice with off-diagonal impurities has been calculated in [19–26].

The quantum correction to the conductivity is calculated according to the Kubo expression

$$\sigma_{\alpha,\beta}(\omega) = i \frac{Ne^2}{m\omega} \delta_{\alpha\beta} + \frac{2e^2}{\omega} \int \frac{d\epsilon}{2\pi} \int \frac{d^2p}{(2\pi)^2} v_\alpha(\mathbf{p}) v_\beta(\mathbf{p}) \langle G(\mathbf{p}, \epsilon + \omega) G(\mathbf{p}, \epsilon) \rangle \quad (32)$$

where  $G(\mathbf{p}, \epsilon)$  is the Green's function and  $v_\alpha(\mathbf{p}) = \frac{\partial \epsilon}{\partial p_\alpha}$  with  $\alpha = (x, y)$  is a component of the electron velocity; the bracket  $\langle \dots \rangle$  denotes averaging over the impurity realizations.

Far from the half-filled energy band, maximally crossed diagrams with normal scattering are responsible for logarithmic corrections to the conductivity of the 2D weakly disordered non-interacting electron gas.<sup>7</sup> These diagrams can be redrawn as a ladder series in the particle-particle channel as shown in Fig.7a.

Bragg reflection is intensified as half-filling is approached. In this case, an act of electron scattering on an impurity may be accompanied by Bragg reflection on the Brillouin zone boundary. The new diagrams which give a contribution to the conductivity as half-filling is approached are drawn in Figs.7b-d'.

The contribution of the diagrams in Fig.6a to the conductivity,  $\delta\sigma_a(\omega)$  can be expressed as follows according to the Kubo expression Eq.(32):

$$\delta\sigma_a(\omega) = \frac{2e^2}{\omega} \int \frac{d\epsilon}{2\pi} \int \frac{d^2p}{(2\pi)^2} C_N(\mathbf{q}, \epsilon, \omega) A_\alpha^N(\mathbf{q}, \epsilon, \omega) \quad (33)$$

where  $C_N(\mathbf{q}, \epsilon, \omega)$  is the cooperon block Eq.(8) for normal scattering and

$$A_\alpha^N(\mathbf{q}, \epsilon, \omega) = \int \frac{d^2p}{(2\pi)^2} v_\alpha(\mathbf{p}) v_\alpha(-\mathbf{p} + \mathbf{q}) G(\mathbf{p}, \epsilon + \omega) G(-\mathbf{p} + \mathbf{q}, \epsilon + \omega) G(\mathbf{p}, \epsilon) G(-\mathbf{p} + \mathbf{q}, \epsilon) \quad (34)$$

For a tight-binding model with nearest-neighbor hopping, the  $\alpha = (x, y)$  component of the velocity  $v_\alpha(\mathbf{p})$  is given as  $v_\alpha(\mathbf{p}) = ta \sin(p_\alpha a)$ . The integration over  $\mathbf{p}$  can be written as  $\int \frac{d\mathbf{S}}{(2\pi)^2 |\mathbf{v}_p|} \int d\xi$ , and then the integral over the energy variable  $\xi$  is done easily. The van Hove singularity, arising at saddle points of the Fermi surface for the half-filled band when  $|\mathbf{v}_p| = ta \sqrt{\sin^2 p_x a + \sin^2 p_y a}$  vanishes, is removed due to the  $v_\alpha^2(\mathbf{p})$  term under the integral over the Fermi surface  $d\mathbf{S}$ . Therefore the value of  $A_\alpha(q, \epsilon, \omega)$  does not strongly differ from that for the free-electron gas model and we get

$$A_\alpha(\mathbf{q}, \epsilon, \omega) = -p_F \tau^2 l \Theta(-\epsilon(\epsilon + \omega)) \quad (35)$$

Using Eqs.(8) and (35) for  $C_N(\mathbf{q}, \epsilon, \omega)$  and  $A_\alpha(\mathbf{q}, \epsilon, \omega)$  in Eq.(33) one gets

$$\delta\sigma_a(\omega) = -\frac{e^2 \tau}{2\pi^2 \tau_N} \ln\left(\frac{1}{\frac{\tau}{\tau_\pi} - i|\omega|\tau}\right) \quad (36)$$

Far from half-filling and far from other commensurate points the Bragg reflection is weakened and  $\tau \approx \tau_N \ll \tau_\pi$ . Therefore  $\delta\sigma_a(\omega)$  in this case represents the conventional weak localization correction to the conductivity.<sup>7</sup>  $\delta\sigma_a(\omega)$  is reduced close to half-filling when umklapp scatterings are enhanced and  $\tau \approx \tau_\pi \ll \tau_N$ .

The diagrams which give an essential contribution to the conductivity at half-filling are shown in Fig.7b-7d'. The appearance of these new diagrams is due to intensified scattering in the  $\pi$ -channel with large momentum transfer. The main quantum correction to the diffusion coefficient at half-filling comes from the “fan” diagrams in Fig.7b with the  $\pi$ -cooperon block. The expression corresponding to this diagram is

$$\delta\sigma_b(\omega) = \frac{2e^2}{\omega} \int \frac{d\epsilon}{2\pi} \int \frac{d^2q}{(2\pi)^2} C_\pi(\mathbf{q}, \epsilon, \omega) A_\pi(\mathbf{q}, \epsilon, \omega) \quad (37)$$

where  $C_\pi(\mathbf{q}, \epsilon, \omega)$  is the  $\pi$ -cooperon given by Eq.(12) and

$$A_\pi(\mathbf{q}, \epsilon, \omega) = \int \frac{d^2p}{(2\pi)^2} v_\alpha(\mathbf{p}) v_\alpha(-\mathbf{p} + \mathbf{q} + \mathbf{Q}_0) G(\mathbf{p}, \epsilon + \omega) G(\mathbf{p}, \epsilon) G(-\mathbf{p} + \mathbf{q} + \mathbf{Q}_0, \epsilon) G(-\mathbf{p} + \mathbf{q} + \mathbf{Q}_0, \epsilon + \omega) \quad (38)$$

The calculation of Eq.(38) is similar to that for  $A_N(\mathbf{q}, \epsilon, \omega)$ . Taking into account the condition that  $v_\alpha(\mathbf{k} + \mathbf{Q}_0) = -v_\alpha(\mathbf{k})$  we obtain the result for  $A_\pi(\mathbf{q}, \epsilon, \omega)$

$$A_\pi(\mathbf{q}, \epsilon, \omega) = \frac{p_F l \tau^2}{(1 - 2i\tau|\epsilon|)(1 - 2i\tau|\epsilon + \omega|)} \left\{ \frac{1}{1 - i\tau|2\epsilon + \omega|} \Theta(\epsilon(\epsilon + \omega)) + \Theta(-\epsilon(\epsilon + \omega)) \right\} \quad (39)$$

Substituting Eqs.(12) and (39) in Eq.(37), the expression for  $\delta\sigma_b(\omega)$  can be reduced by some simple calculations to

$$\delta\sigma_b(\omega) = \frac{e^2 \tau}{2\pi^2 \omega \tau_\pi} \left\{ \left( \frac{\tau}{\tau_\pi} \right)^2 I\left( \frac{\tau}{\tau_\pi}, \omega\tau \right) + \frac{\omega}{2} \right\} \quad (40)$$

with

$$\begin{aligned} I\left( \frac{\tau}{\tau_\pi}, \bar{\omega} = \omega\tau \right) &= \frac{i}{2\tau} \int_0^1 dx \int_0^\infty dz \frac{1}{(z+i)^3} \frac{1}{(z + \bar{\omega} + i)^2 - x + \left( \frac{\tau}{\tau_\pi} \right)^2} \\ &= \frac{i}{4\tau} \left\{ 2i\bar{\omega} \left[ \frac{1}{\bar{\omega}^2 - 1 + \left( \frac{\tau}{\tau_\pi} \right)^2} - \frac{1}{\bar{\omega}^2 + \left( \frac{\tau}{\tau_\pi} \right)^2} \right] + \left[ 1 + \frac{1}{(\bar{\omega} - \sqrt{1 - \left( \frac{\tau}{\tau_\pi} \right)^2})^2} \right] \ln(1 - i\bar{\omega} + i\sqrt{1 - \left( \frac{\tau}{\tau_\pi} \right)^2}) \right. \\ &\quad + \left[ 1 + \frac{1}{(\bar{\omega} + \sqrt{1 - \left( \frac{\tau}{\tau_\pi} \right)^2})^2} \right] \ln(1 - i\bar{\omega} - i\sqrt{1 - \left( \frac{\tau}{\tau_\pi} \right)^2}) + \left[ \frac{1}{\left( \frac{\tau}{\tau_\pi} - i\bar{\omega} \right)^2} - 1 \right] \ln(1 - i\bar{\omega} + \frac{\tau}{\tau_\pi}) \\ &\quad \left. + \left[ \frac{1}{\left( \frac{\tau}{\tau_\pi} + i\bar{\omega} \right)^2} - 1 \right] \ln(1 - i\bar{\omega} - \frac{\tau}{\tau_\pi}) \right\} \end{aligned} \quad (41)$$

The expression for  $\delta\sigma_b(\omega)$  can be presented for two limiting cases, namely near the middle of the band when  $\tau \approx \tau_\pi \ll \tau_N$  and far from half-filling when  $\tau \approx \tau_N \ll \tau_\pi$  by using Eq.(41) in (40):

$$\delta\sigma_b(\omega) = \begin{cases} \frac{e^2}{4\pi^2} \ln(1 - \frac{\tau}{\tau_\pi} - i\omega\tau) + i \frac{e^2}{8\pi^2 \omega \tau_\pi} & \text{for } \frac{\tau}{\tau_\pi} \rightarrow 1 \\ \text{const} + i \frac{e^2}{4\pi^2 \omega \tau_\pi} \left( \frac{\tau}{\tau_\pi} \right)^2 \ln 2 & \text{for } \frac{\tau}{\tau_\pi} \approx \frac{\tau_N}{\tau_\pi} \rightarrow 0 \end{cases} \quad (42)$$

So the quantum correction to the conductivity corresponding to the diagram in Fig.7b decreases  $\sigma(\omega)$  logarithmically with the external frequency near half-filling. The contribution of Fig.7b vanishes through a small offset from the middle of the band.

Analyzing the effect of substitutional impurities on the conductivity by means of the diffusion coefficient, which is expressed by the diagrams a) and b) in Fig.7, it can be seen that the logarithmic correction to the localization correction to  $\sigma(\omega)$  is preserved irrespectively of the band filling. However, the coefficient of the logarithm of the quantum correction to the conductivity is changed from  $\frac{e^2}{2\pi^2}$  in Eq.(36) far from half-filling to  $\frac{e^2}{4\pi^2}$  in Eq.(42) close to half-filling. On the other hand, the  $\pi$ -scattering mechanism gives a perturbative contribution to the dielectric constant  $\epsilon'(\omega) \sim \text{Im}\sigma(\omega)$ . The contribution to  $\epsilon'(\omega)$  increases close to half-filling. This also means that there exist a few delocalized states at the center of the band.

The diagrams in Fig.7c-d' represent the quantum correction to the conductivity due to changes in the DOS. The expression corresponding to the sum of these diagrams can be presented as

$$2(\delta\sigma_c(\omega) + \delta\sigma_d(\omega)) = \frac{2e^2}{\omega} \int \frac{d\epsilon}{2\pi} \int \frac{d^2 q}{(2\pi)^2} \alpha(\mathbf{q}, \epsilon + \omega) B(\mathbf{q}, \epsilon, \omega) \quad (43)$$

where

$$\alpha(\mathbf{q}, \epsilon) = C_\pi(\mathbf{q}, \epsilon) - \frac{2\tau}{\tau_\pi} \left( 1 - \frac{\tau}{\tau_\pi} \right) D_\pi(\mathbf{q}, \epsilon) \quad (44)$$

and

$$B(\mathbf{q}, \epsilon, \omega) = \frac{p_F l \tau^2}{(1 - 2i\tau|\epsilon + \omega|)^2} \left\{ \left( \frac{\tau}{\tau_N} - 2 \right) \Theta(-\epsilon(\epsilon + \omega)) + \frac{1}{1 - i\tau|\epsilon + \omega| - i\tau|\epsilon|} \Theta(\epsilon(\epsilon + \omega)) \right\} \quad (45)$$

The fact that the contributions from diagrams c' and d' in Fig.7 are equal to those from c and d is taken into account in Eq.(43). The cooperon and diffusion insertions into the Green's function are given by Eqs.(18) and (19), respectively.

After some routine calculations, Eq.(43) for the correction to the conductivity due to the DOS is reduced to the form

$$2(\delta\sigma_c(\omega) + \delta\sigma_d(\omega)) = \frac{e^2\tau^3}{2\pi^2\omega\tau_\pi^3} \left[ 1 - \frac{2\tau}{\tau_\pi} \left( 1 - \frac{\tau}{\tau_\pi} \right) \right] \left\{ I\left(\frac{\tau}{\tau_\pi}, \bar{\omega} = \omega\tau\right) + \frac{\omega}{2} \left( \frac{\tau}{\tau_N} - 3 \right) \ln \frac{1 - \left(\frac{\tau}{\tau_\pi}\right)^2 + (1 - 2i\omega\tau)^2}{(1 - 2i\omega\tau)^2 + \left(\frac{\tau}{\tau_\pi}\right)^2} \right\} \quad (46)$$

Where  $I(\frac{\tau}{\tau_\pi}, \bar{\omega} = \omega\tau)$  is given by Eq.(41). These contributions vanish as expected far from half-filled band, when  $\tau_\pi \gg \tau \approx \tau_N$ . However, they give a large contribution to the conductivity near half-filling,  $\tau \approx \tau_\pi \ll \tau_N$ , giving rise to a rapid increasing of the conductivity with the external frequency. So, the total contribution to the conductivity is obtained by summing Eqs.(36), (42), and (46). Far from half-filling, only the normal cooperon gives a contribution and, as a result  $\delta\sigma_a(\omega)$  survives:

$$\delta\sigma(\omega) = -\frac{e^2}{2\pi^2} \ln\left(-\frac{1}{i|\omega|\tau}\right) \quad (47)$$

The quantum correction to the conductivity near half-filling is due to the  $\pi$ -cooperon and

$$\delta\sigma(\omega) = -\frac{5e^2}{2\pi^2} \ln\left(-\frac{1}{i|\omega|\tau_\pi}\right) \quad (48)$$

with  $\tau \rightarrow \tau_\pi$ . Although the conductivity decreases with the external frequency, the diffusion coefficient increases with approaching half-filling for given  $\omega$ , which means a partial lifting of localization at the center of the band due to a few delocalized states. The rapid decrease of the conductivity (Eq.(48)) near half-filling is the result of the impurity effect on the DOS.

## V. CONCLUSION

The character of localization in the 2D disordered electronic gas has been a subject of debate for a long time. The question whether delocalized states exist in the center of the band of 2D disordered systems or not is also one of the crucial points for the integer quantum Hall effect.

Searches for delocalized states have been mainly concentrated around the 2D Anderson model. Expectations are connected with the existence of the van Hove singularity in the band center of the square lattice, which might give rise to a delocalization of states at half-filling. Various numerical approaches have been applied to compute the DOS,<sup>27,28</sup> the localization length,<sup>35,36,28,37,29</sup> and the conductivity<sup>34,38</sup> of the 2D Anderson model with diagonal and off-diagonal disorder. The computations show that although even a small concentration of diagonal disorder suppresses the van Hove singularity, off-diagonal disorder preserves it, however with a modified shape.

The exponential localization of all states for diagonal disorder<sup>38,36</sup> has been revealed by computational approaches whereas the existence of quasi-localized states has been predicted for the 2D Anderson model with off-diagonal disorder.<sup>35,28,37</sup> In other words, the computation of the effects of off-diagonal disorder provides evidence for the transformation from exponential to power-like localization as half-filling is approached.

In this paper we tried to give a complete picture for the DOS and the conductivity, and also to give some physical insight into the processes occurring near half-filling in simple lattices with substitutional impurities.

The impurity concentration is considered to be small, so that the condition  $\epsilon_F\tau \gg 1$  or  $p_Fl \gg 1$  is satisfied and the weak localization approximation is applicable.

Apart from normal scattering with small momentum transfer, umklapp scattering with large momentum transfer is shown to be essential near half-filling. This new scattering involves coherent reflection of an electron on the boundary of the Brillouin zone for each act of scattering.

Our diagrammatical approach shows that the new singular blocks, namely the  $\pi$ -cooperon  $C_\pi(\mathbf{q}, \epsilon, \omega)$  and the  $\pi$ -diffuson  $D_\pi(\mathbf{k}, \epsilon, \omega)$ , give a large contribution to the DOS and the conductivity at half-filling. The dependence of the DOS on the energy and the impurity strength near the middle of the band have been determined by summing the leading logarithmically divergent contributions. The results obtained [Eqs.(27) and (30)] for the DOS show that weak disorder due to substitutional impurities does not remove the van Hove singularity at the center of the 2D band. However its energy dependence is strongly changed. The impurity effect on the 3D DOS is a shallow dip on the smooth background of the bare DOS in the middle of the band.

The effect might be observable in the temperature dependence of the magnetic susceptibility according to

$$\chi_{(d)}(T) = 2\mu_B^2 \int \frac{d\epsilon}{4T} \cosh^{-2}\left(\frac{\epsilon}{2T}\right) \rho^{(d)}(\epsilon) \quad (49)$$

Where  $\mu_B$  is the Bohr magneton. Straightforward calculation using Eq.(27) for the 2D DOS gives

$$\chi_{2D}(T) \propto \ln^{1/2}\left(\frac{1}{T\tau_\pi}\right)$$

For  $d = 3$ , the correction to the magnetic susceptibility can again be calculated according to Eqs.(49) and (30). However, this correction is negligibly small.

The first logarithmic corrections to the conductivity of the 2D square lattice with substitutional impurities come from both the diffusion coefficient and the DOS. The corrections due to the diffusion coefficient,  $\delta\sigma_a(\omega) + \delta\sigma_b(\omega)$ , given by Eqs.(36) and (42), decrease in magnitude as half-filling is approached while they remain logarithmically dependent on the external frequency. Such a partial lifting of localization may be due to a few delocalized states in the center of the band.<sup>35,36,28,37,29</sup> The imaginary part of  $\sigma(\omega)$ , which corresponds to the dielectric constant, increases close to half-filling. This fact supports the picture of an increase of the electronic mobility at the center of the band.

Nevertheless, the contribution to  $\sigma(\omega)$  due to the DOS suppresses the relative increase in the conductivity coming from the diffusion coefficient.

- <sup>1</sup> S. V. Kravchenko *et al.*, Phys. Rev. B **50**, 8039 (1994).
- <sup>2</sup> P. Mohanty, E. M. Q. Jariwala, and R. A. Webb, Phys. Rev. Lett. **78**, 3366 (1997).
- <sup>3</sup> I. M. Lifshits, S. A. Gredeskul, and L. A. Pastur, *Introduction to the theory of disordered systems* (Wiley, New York, 1988).
- <sup>4</sup> E. Abrahams, P. W. Anderson, D. C. Licciardello, and T. V. Ramakrishnan, Phys. Rev. Lett. **42**, 673 (1979).
- <sup>5</sup> V. L. Berezinskii, Zh. Eksp. Teor. Fiz. **65**, 1251 (1973), [Sov. Phys. JETP **38**, 620, 1974].
- <sup>6</sup> N. F. Mott and W. D. Twose, Adv. Phys. **10**, 107 (1961).
- <sup>7</sup> L. P. Gorkov, A. I. Larkin, and D. E. Khmel'nitskii, Pis'ma Zh. Eksp. Teor. Fiz. **30**, 248 (1979), [JETP Lett. **30**, 228 (1979)].
- <sup>8</sup> B. L. Altshuler and A. G. Aronov, in *Electron-Electron Interactions in Disordered Systems*, edited by A. L. Efros and M. Pollak (Elsevier, North-Holland, 1985), Chap. Electron-Electron Interaction In Disordered Conductors.
- <sup>9</sup> B. L. Altshuler, A. G. Aronov, and P. A. Lee, Phys. Rev. Lett. **44**, 1288 (1980).
- <sup>10</sup> H. Fukuyama, in *Electron-Electron Interactions in Disordered Systems*, edited by A. L. Efros and M. Pollak (Elsevier, North-Holland, 1985), Chap. Electron-Electron Interaction in Condensed Matter.
- <sup>11</sup> P. A. Lee and T. V. Ramakrishnan, Rev. Mod. Phys. **57**, 287 (1985).
- <sup>12</sup> M. Pollak, Discuss. Faraday. Soc. **50**, 13 (1970).
- <sup>13</sup> A. L. Efros and B. I. Shklovskii, J. Phys. C **8**, L49 (1975).
- <sup>14</sup> B. I. Shklovskii and A. L. Efros, *Electronic properties of doped semiconductors*, Springer Series in Solid State Sciences (Springer, New York, 1984).
- <sup>15</sup> E. P. Nakhmedov, M. Kumru, and R. Oppermann, Phys. Rev. Lett. (submitted) .
- <sup>16</sup> A. A. Abrikosov, L. P. Gorkov, and I. E. Dzyaloshinski, *Methods of Quantum Field Theory in Statistical Physics* (Dover, New York, 1963).
- <sup>17</sup> N. W. Ashcroft and N. D. Mermin, *Solid State Physics* (Saunders College, Fort Worth, 1975).
- <sup>18</sup> F. J. Dyson, Phys. Rev. **92**, 1331 (1953).
- <sup>19</sup> M. Weissmann and N. V. Cohan, J.Phys.C:Solid State Phys. **8**, 109 (1975).
- <sup>20</sup> L. P. Gorkov and O. N. Dorokhov, Solid State Commun. **20**, 789 (1976).
- <sup>21</sup> A. A. Ovchinnikov and N. S. Erikhman, Pis'ma v Zh. Eksp. Teor. Fiz. **25**, 197 (1977), [ Sov. Phys. JETP Lett. **25**, 180 (1977)].
- <sup>22</sup> A. A. Gogolin and V. I. Melnikov, Zh. Eksp. Teor. Fiz. **73**, 706 (1977), [Sov. Phys. JETP **46**, 369, 1977].
- <sup>23</sup> S. A. Gredeskul and L. A. Pastur, Zh. Eksp. Teor. Fiz. **75**, 1444 (1987), [Sov. Phys. JETP **48**, 729 (1978)].
- <sup>24</sup> J. E. Hirsch and T. P. Eggarter, Phys.Rev. B **14**, 2433 (1976).
- <sup>25</sup> T. P. Eggarter and R. Riedinger, Phys. Rev. B **18**, 569 (1978).
- <sup>26</sup> M. Inui, S. A. Trugman, and E. Abrahams, Phys. Rev. B **49**, 3190 (1994).
- <sup>27</sup> W. M. Hu, J. D. Dow, and C. W. Myles, Phys. Rev. B **30**, 1720 (1984).
- <sup>28</sup> A. Eilmes, R. Römer, and M. Schreiber, Eur. Phys. J. B **1**, 29 (1998).
- <sup>29</sup> B. Kramer and A. M. Kinnon, Rep. Prog. Phys. **56**, 1969 (1993).

- <sup>30</sup> R. Oppermann and F. Wegner, Z. Phys. B **34**, 327 (1979).
- <sup>31</sup> B. L. Altshuler, V. E. Kravtsov, and I. V. Lerner, Zh. Eksp. Teor. Fiz. **91**, 2276 (1986), [Sov. Phys. JETP **64**, 1352 (1986)].
- <sup>32</sup> G. Bergmann, Phys. Rev. B **28**, 2914 (1983).
- <sup>33</sup> J. Ruvalds *et al.*, Phys. Rev. B **51**, 3797 (1995).
- <sup>34</sup> J. Stein and U. Krey, Z. Phys. B **37**, 13 (1980).
- <sup>35</sup> C. M. Soukoulis, I. Webman, G. S. Grest, and E. N. Economou, Phys. Rev. B **26**, 1838 (1982).
- <sup>36</sup> A. M. Kinnon and B. Kramer, Z. Phys. B - Condens. Matter **53**, 1 (1983).
- <sup>37</sup> A. Eilmes, R. Römer, and M. Schreiber, phys. stat. sol. (b) **205**, 229 (1998).
- <sup>38</sup> P. A. Lee and D. S. Fisher, Phys. Rev. Lett. **47**, 882 (1981).